

Assembly and Disassembly of the Capsid-Like External Scaffold of Immature Virions during Vaccinia Virus Morphogenesis[▽]

Himani Bisht, Andrea S. Weisberg, Patricia Szajner, and Bernard Moss*

Laboratory of Viral Diseases, National Institute of Allergy and Infectious Diseases, National Institutes of Health, Bethesda, Maryland 20892-3210

Received 30 April 2009/Accepted 19 June 2009

Infectious poxvirus particles are unusual in that they are brick shaped and lack symmetry. Nevertheless, an external honeycomb lattice comprised of a capsid-like protein dictates the spherical shape and size of immature poxvirus particles. In the case of vaccinia virus, trimers of 63-kDa D13 polypeptides form the building blocks of the lattice. In the present study, we addressed two questions: how D13, which has no transmembrane domain, associates with the immature virion (IV) membrane to form the lattice structure and how this scaffold is removed during the subsequent stage of morphogenesis. Interaction of D13 with the A17 membrane protein was demonstrated by immunoaffinity purification and Western blot analysis. In addition, the results of immunogold electron microscopy indicated a close association of A17 and D13 in crescents, as well as in vesicular structures when crescent formation was prevented. Further studies indicated that binding of A17 to D13 was abrogated by truncation of the N-terminal segment of A17. The N-terminal region of A17 was also required for the formation of crescent and IV structures. Disassembly of the D13 scaffold correlated with the processing of A17 by the I7 protease. When I7 expression was repressed, D13 was retained on aberrant virus particles. Furthermore, the morphogenesis of IVs to mature virions was blocked by mutation of the N-terminal but not the C-terminal cleavage site on A17. Taken together, these data indicate that A17 and D13 interactions regulate the assembly and disassembly of the IV scaffold.

The assembly and morphogenesis of vaccinia virus (VACV) and other poxviruses occurs in specialized regions of the cytoplasm called factories. The first distinctive viral forms discerned by transmission electron microscopy are spherical immature virions (IVs) and their membrane crescent precursors, which appear to be covered by a layer of spicules (14). More-recent studies employing three-dimensional deep-etch electron microscopy revealed that the “spicule coat” of IVs is actually a continuous honeycomb lattice (20). The IVs enclose dense granular material comprising the core precursors and a DNA nucleoid. The “spicule coat” is lost as the IVs undergo a remarkable transition into dense, brick-shaped infectious mature virions (MVs).

Several studies led to the identification of D13 protein trimers as the building blocks of the scaffold: (i) single amino acid changes in D13 are responsible for VACV mutants that are resistant to the drug rifampin (rifampicin) (4, 11, 42), which causes reversible formation of irregular membranes lacking the “spicule coat” (18, 29, 30); (ii) repression of D13 expression results in a phenotype identical to that caused by the drug rifampin (50); (iii) antibody to D13 labels IVs (40) on the outer surface (28, 41); (iv) in the presence of rifampin, D13 antibodies label cytoplasmic inclusions that are distinct from aberrant viral membranes (40); and (v) the results of physical and microscopic studies indicate that D13 exists as trimers of 63-kDa subunits arranged mostly in hexagons on the surface of IVs (41).

Poxviruses are thought to share a common origin with mem-

bers of the asfarvirus, iridovirus, phycodnavirus, and mimivirus families (23). These large DNA viruses, except for the poxviruses, have an icosahedral capsid surrounding an internal membrane (31, 47–49). Interestingly, a domain of VACV D13 has homology with the capsid proteins of these related large DNA viruses (24). Moreover, a parapoxvirus ortholog of D13 was shown to self-assemble in vitro and to have structural similarities with the capsid proteins (22). These findings, together with the honeycomb lattice structure of the IV scaffold, suggest that the infectious form of the ancestor of poxviruses may have had an icosahedral capsid and that the stages of morphogenesis recapitulate evolution (41).

In the present study, we addressed two questions: how D13, which has no transmembrane domain, associates with the IV membrane to form the lattice structure and how the scaffold is removed during morphogenesis.

MATERIALS AND METHODS

Cells and viruses. BS-C-1 and HeLa cells were maintained in Eagle's minimum essential medium and Dulbecco's modified Eagle's medium (Quality Biologicals, Gaithersburg, MD) supplemented with 10% fetal bovine serum. VACV (WR strain) and recombinant viruses were propagated and titrated as described previously (17).

Antibodies. The following rabbit anti-peptide sera were used: D13 (B1), against amino acids 536 to 550 of the D13 open reading frame (ORF) (40); A17N, against amino acids 26 to 37 of the A17 ORF (7); A17C, against the last 12 amino acids of the A17 ORF (46); and H3, against amino acids 247 to 259 of the H3 ORF (12). Rabbit antibodies to A28 (32) and L1 (27) were raised against secreted forms made in insect cells, or in the case of A14, rabbit antibody was raised to a fusion protein made in *Escherichia coli* (43). Anti-V5 mouse monoclonal antibody, clone V5-10 conjugated to agarose beads, was from Sigma (St. Louis, MO).

Plasmids. pCDNA3.1-V5-D13 was made by inserting the D13 ORF tagged with the V5 coding sequence at the 5' end and regulated by a bacteriophage T7 promoter. The full-length A17 and truncated forms were made by amplifying the

* Corresponding author. Mailing address: National Institutes of Health, 33 North Drive, Bethesda, MD 20892-3210. Phone: (301) 496-9869. Fax: (301) 480-1535. E-mail: bmoss@nih.gov.

▽ Published ahead of print on 1 July 2009.

A17 ORF with specific primers and inserting them between the NcoI and BamHI sites of pVOTE1 (44) modified to encode enhanced green fluorescent protein (GFP) instead of xanthine-guanine phosphoribosyltransferase (16). Plasmids encoding the full-length A17 ORF and deletion mutants regulated by the natural A17 promoter were also cloned, using a Zero blunt TOPO PCR cloning kit (Invitrogen, Carlsbad, CA).

Immunoaffinity purification. Cells were lysed in 50 mM Tris-HCl, pH 8.0, 150 mM NaCl, 1% NP-40, 0.1% sodium dodecyl sulfate (SDS), and protease inhibitor cocktail tablets (Roche Applied Science, Indianapolis, IN) at 4°C for 30 min. Cleared lysates were incubated overnight at 4°C with anti-V5 agarose beads (Sigma). The beads were washed and then subjected to SDS-polyacrylamide gel electrophoresis (PAGE) and Western blotting essentially as described previously (8).

Complementation assay. HeLa cells were infected with vA17Li (45) at a multiplicity of 3 or 5 PFU per cell in the absence of isopropyl β-D-1-thiogalactopyranoside (IPTG) for 1 h. The cells were washed and transfected with plasmid(s) by using Lipofectamine 2000 (Invitrogen) in Opti-MEM I reduced medium (Invitrogen). The medium was replaced with fresh Eagle's minimal essential medium containing 2.5% fetal bovine serum after 4 to 5 h. After approximately 24 h, the cells were harvested and freeze-thawed three times, and the virus titers were determined by plaque assay in the presence of IPTG.

Electron microscopy. For conventional transmission electron microscopy, infected BS-C-1 cells in 60-mm-diameter wells were fixed with 2% glutaraldehyde and embedded in EmBed-182 resin (Electron Microscopy Sciences, Hatfield, PA). Procedures for cryosectioning and immunogold labeling were described previously (39). Double-label experiments with rabbit antibodies were carried out as follows. Grids were incubated with a 1:100 or 1:200 dilution of the first rabbit antibody in 1% fish skin gelatin in 0.1 M phosphate, pH 7.4 buffer at room temperature in the dark and washed with 0.1% fish skin gelatin four times for 1 min and once for 2 min. The grids were then incubated with protein A-gold in 1% fish skin gelatin in phosphate buffer for 45 min at room temperature in the dark. The grids were placed in 1% glutaraldehyde in phosphate buffer for 5 min and then washed twice for 5 min with phosphate buffer. The procedure was then repeated with the second rabbit antibody, using protein conjugated to another size of gold. To confirm the specificity of labeling with the two sizes of gold, each experiment was done with at least four permutations in which both antibodies were used, the first antibody was omitted, the second antibody was omitted, or both antibodies were omitted. In addition, the order of the first and second antibodies was switched. Specimens were viewed with FEI-CM100 and FEI Tecnai Spirit transmission electron microscopes (FEI, Hillsboro, OR).

RESULTS

Association of D13 scaffold protein with the A17 viral membrane protein. We considered that the association of the D13 scaffold protein with the IV might occur through physical interaction with a transmembrane protein. Of the IV membrane proteins, A17 and A14 seemed possible candidates. A17 is essential for the formation of crescents and IVs, which contain the D13 outer scaffold (34, 45). When A17 is repressed, only heterogeneous vesicular and tubular structures are observed. More-regular vesicular structures form when A14 is repressed; however, some crescents and IVs can be detected under these conditions (37, 43). Immunoaffinity purification experiments were carried out to determine whether D13 associates with A17, A14, or other proteins. Cells were infected with vV5D13, a replication-competent VACV that expresses D13 with a V5 epitope tag at its N terminus (41), or with unmodified VACV as a control. The cells were lysed with detergent to disrupt membranes, and the clarified lysate was incubated with anti-V5 immunoglobulin G-conjugated agarose beads. The bound proteins were analyzed by SDS-PAGE followed by Western blotting with antibodies to individual VACV membrane proteins. Bands corresponding to processed and unprocessed forms of A17 were detected in the bound proteins from lysates of cells infected with vV5D13 but not from cells infected with the control strain WR virus lacking the V5 epitope tag on D13

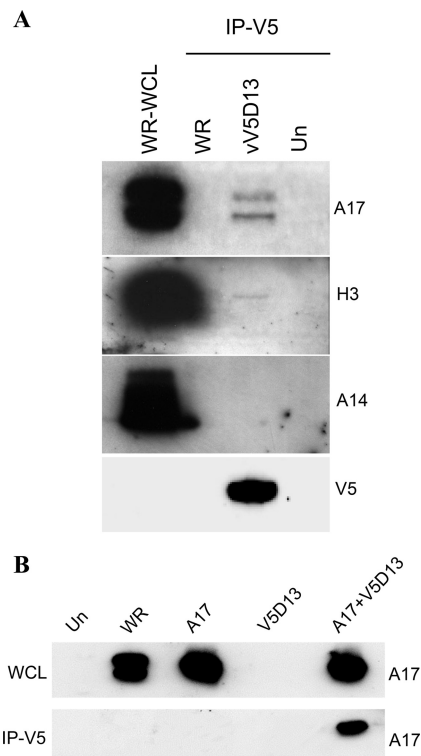


FIG. 1. (A) Coimmunoprecipitation of VACV membrane proteins with epitope-tagged D13. BS-C-1 cells that were uninfected (Un) or infected for 24 h with wild-type VACV (WR) or virus with V5-tagged D13 (vV5D13) were lysed in buffer containing 1% NP-40 and 0.1% SDS, and clarified whole-cell lysates were either analyzed directly by SDS-PAGE (WR-WCL) or first bound and eluted from V5 antibody conjugated to beads (IP-V5). Western blotting was carried out with A17N, H3, A14, and V5 antibodies. (B) Interaction of D13 with A17 in the absence of other viral late proteins. Cells were uninfected (Un), infected with wild-type VACV (WR), or in all other lanes, infected with a recombinant VACV (vTF7-3) in the presence of AraC and transfected with plasmid encoding wild-type A17 (A17) or V5-tagged D13 (V5D13) or both (A17+v5D13). After 24 h, the cells were lysed and subjected directly to SDS-PAGE (WCL) or immunoaffinity purified using anti-V5-conjugated agarose beads (IP-V5). The Western blotting was performed with rabbit anti-A17N.

(Fig. 1A). The faster-migrating A17 band has lost a short C-terminal segment by proteolytic processing, but the N-terminal 16-amino-acid segment may still be present (7, 25). A faint band of the correct size was also detected when the bound proteins were analyzed with antibody to the H3 membrane protein (Fig. 1A). However, this association was considered less relevant than the A17 interaction since IVs can form in the absence of H3 (13, 26). A14 was not detected among the bound proteins (Fig. 1A), even though A14 and A17 are associated under some circumstances (7, 36). Whether A14 interacts directly or indirectly with A17 is not known. Two other membrane proteins, L1 and A28, were not detected among proteins that bound to V5D13 (data not shown). L1 and A28 are not required for virion assembly but have roles in virus entry (8, 38).

Further experiments were designed to confirm the association of D13 and A17 and to determine whether this interaction is direct or mediated through another viral late protein. To

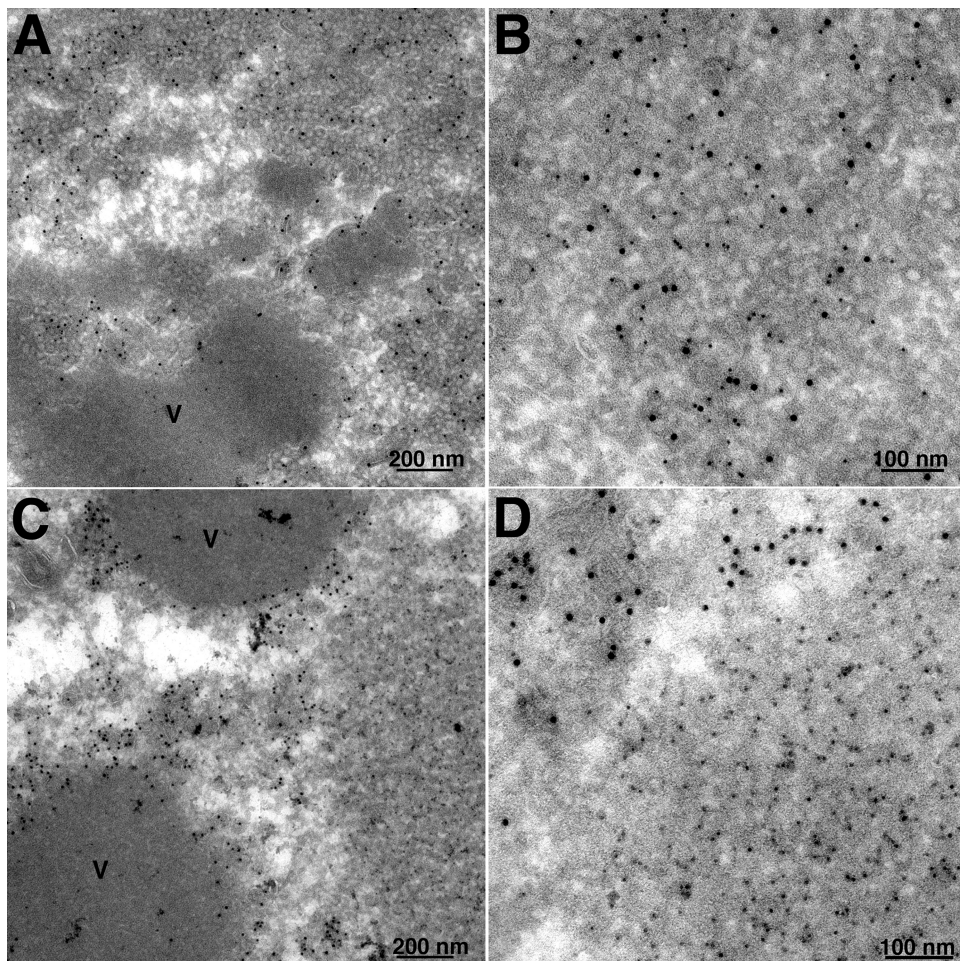


FIG. 2. Localization of A17 and D13 by immunoelectron microscopy. Cells were infected with 3 PFU per cell of an A14-inducible VACV in the absence of doxycycline (A, B) or an A17-inducible VACV (vA17Li) in the absence of IPTG (C, D). After 24 h, cells were fixed, cryosectioned, and double stained with anti-D13 and anti-A17 (A, B) and anti-A14 (C, D) antibodies followed by secondary antibodies and protein A conjugated to 5- and 10-nm colloidal gold, respectively. V, dense viroplasm.

investigate the latter, cytosine arabinoside (AraC) was used to prevent viral genome replication needed for intermediate and late gene expression. The AraC-treated cells were infected with vTF7-3, a recombinant VACV that expresses bacteriophage T7 RNA polymerase from an early promoter, and transfected with plasmids encoding A17- and V5-tagged D13 regulated by T7 promoters. Under these conditions, the only viral late proteins expressed are the V5-tagged D13 and A17. The cells were lysed after 24 h, and proteins captured with anti-V5-conjugated agarose. The specific association of A17 with D13 was demonstrated by Western blotting with anti-A17 antibody (Fig. 1B). Note that only the higher-molecular-weight precursor form of A17 was detected because the I7 protease was not made in the presence of AraC. Thus, the D13-A17 interaction did not require other viral late proteins, some of which are needed for viral membrane formation. It is likely that under these conditions, A17 is inserted into membranes of the intermediate compartment (25, 36) or the endoplasmic reticulum (21). Thus, it is possible that the interaction of D13 and A17 occurred on cellular membranes or postlysis, i.e., after the addition of detergent. Regardless of where the interaction

occurred, the data support the specific interaction of the two proteins.

Colocalization of D13 and A17 in the absence of crescents and IVs. Under normal conditions, A17, A14, and D13 are associated with crescent and IV structures. However, as referenced above, vesicular and tubular structures instead of crescent and IV membranes are formed when the synthesis of A17 is repressed and clusters of more-uniform vesicles are seen in the absence of A14. Interestingly, A14 is associated with the structures that form when the synthesis of A17 is repressed (36) and A17 is associated with the vesicles that form when the synthesis of A14 is repressed (43). However, the location of D13 under these conditions has not been investigated. Using a recombinant VACV with an inducible A14 gene, kindly provided by P. Traktman (43), we observed clusters of 22-nm vesicles containing A17 by immunogold staining in the absence of doxycycline inducer and also showed that D13 was present. Double staining with 10-nm gold particles for A17 and 5-nm gold particles for D13 (Fig. 2A and B) and single staining (not shown) were used. In the lower-magnification image (Fig. 2A), the clusters of A17/D13 vesicles can be seen to extend away

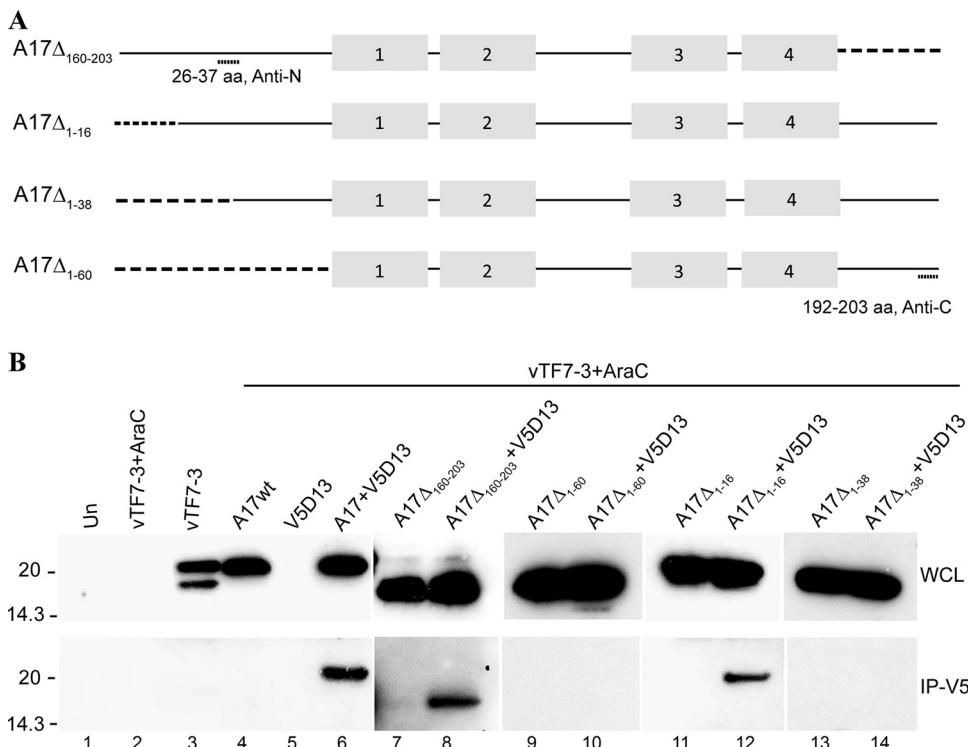


FIG. 3. Effects of A17 truncations on interaction with D13. (A) Diagram of A17 truncation mutants. A17 Δ 160-203 has 44 amino acids deleted from the C terminus; A17 Δ 1-16, A17 Δ 1-38, and A17 Δ 1-60 have 16, 38, and 60 amino acids, respectively, deleted from the N terminus of A17. Truncations are indicated by dashed lines. Antibodies for Western blotting were raised against peptides corresponding to amino acids 26 to 37 (Anti-N) or 192 to 203 (Anti-C). The gray boxes indicate the four α -helical hydrophobic domains. (B) In the lanes under the bar, the samples were obtained from cells that were infected with vTF7-3 in the presence of AraC and transfected with plasmids encoding full-length (wild type) A17 (A17wt) or A17 truncation mutants alone or with V5-tagged D13 as indicated. In the lanes to the left of the bar, samples were from untransfected cells that were uninfected (Un), infected with vTF7-3 in the presence of AraC, or infected with vTF7-3 without AraC. After 24 h, the cells were lysed and subjected directly to SDS-PAGE (WCL) or first bound and then eluted from anti-V5-conjugated agarose beads (IP-V5). Western blotting was performed with rabbit anti-A17N (lanes 1 to 8) or anti-A17C (lanes 9 to 14) and developed by chemiluminescence. Molecular masses (kDa) are shown on the left.

from the electron-dense inclusions of viroplasm. Parallel experiments were carried out using vA17Li, a recombinant VACV with an IPTG-inducible A17 gene (45). In the absence of inducer, A14 (10-nm gold particles) was present in tubulovesicular structures closely associated with the periphery of electron-dense inclusions, but D13 (5-nm gold particles) accumulated in separate depots (Fig. 2C and D). Previous studies had shown that similar depots forming in the presence of rifampin were comprised of 6- to 7-nm D13 trimers (41). These data supported a close association of D13 with A17 even in the absence of crescent and IV structures and were consistent with the results of immunoaffinity purification.

The N-terminal region of A17 is required for binding to D13. A17 is a 203-amino-acid-long protein with four α -helical hydrophobic domains. The N and C termini face the cytoplasm with either two (5, 6) or four (25) membrane-spanning domains. The I7 protease cleaves A17 after glycines 16 and 18 near the N terminus and 185 near the C terminus (2). Based on topology, we expected that D13 would interact with the N- or C-terminal region of A17. To determine the binding region, we constructed expression plasmids containing full-length A17 or the N- or C-terminally truncated forms A17 Δ 1-60 and A17 Δ 160-203 with amino acids 1 to 60 or 160 to 203 deleted, respectively (Fig. 3A). In addition, we made a shorter N-ter-

minal truncation, A17 Δ 1-16, that corresponds to the segment removed by I7 protease, as well as a longer N-terminal truncation, A17 Δ 1-38 (Fig. 3A). In each construct, transcription of the A17 gene was regulated by the T7 promoter. To prevent the expression of genomic A17 and D13, which are regulated by late promoters, the cells were infected with vTF7-3 in the presence of AraC. The infected cells were then transfected with plasmids containing full-length or truncated A17 with or without V5-tagged D13, also regulated by the T7 promoter. Western blots of the transfected cell lysates, carried out with polyclonal antibody raised against a peptide corresponding to amino acids 26 to 37 or amino acids 192 to 203 (Fig. 3A), demonstrated that each mutated form of A17 was expressed (Fig. 3B). The association of V5-tagged D13 with the truncated forms of A17 was analyzed by capturing D13 with anti-V5 antibody beads. D13 was still able to bind A17 after truncation of the C-terminal segment but not after removal of the entire N-terminal segment (Fig. 3B). However, removal of only the first 16 amino acids did not prevent D13 binding, whereas removal of 38 amino acids did (Fig. 3B). Similar results were obtained with influenza virus hemagglutinin-epitope-tagged versions of the A17 mutants when antihemagglutinin antibody rather than rabbit polyclonal anti-A17 was used for Western blotting (data not shown). These data suggested that the bind-

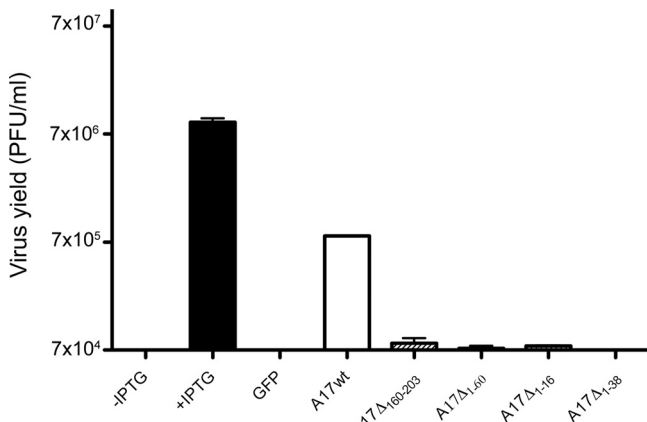


FIG. 4. Complementation of vA17Li infectivity by truncated A17 proteins. Cells were infected with 5 PFU of vA17Li per cell in the presence of IPTG (+IPTG) or the absence of IPTG (all other lanes) and not transfected (first lane) or transfected with plasmids encoding GFP, full-length (wild type) A17, (A17wt), or truncation mutants of A17. After 24 h, virus titers were determined by plaque assay in the presence of 100 μ M IPTG. Error bars show standard deviations.

ing site for D13 includes the segment from amino acid 16 to 38 of A17.

Crescents are not formed when the N-terminal region of A17 is deleted. Additional experiments were carried out to correlate D13 binding to A17 with crescent and IV formation. For these experiments, we infected cells with vA17Li in the absence of inducer to prevent the expression of endogenous A17 and then transfected them with plasmids containing full-length or truncated A17 regulated by the natural A17 promoter. The transfection efficiency was approximately 70% under these conditions, as determined with a plasmid expressing GFP. Only the full-length A17 significantly complemented the VACV mutant's infectivity in the absence of inducer (Fig. 4).

In cells infected with vA17Li and not induced or transfected, vesicles and tubules accumulated in close proximity to the large, electron-dense inclusions of viroplasm (Fig. 5A and B). The absence of more-advanced structures in untransfected cells allowed us to identify those cells that were transfected. Typically about 50 transfected cells were carefully examined, and the structures seen were very consistent for each form of A17. Thus, normal-looking crescents and IVs (Fig. 5C), as well as MVs (Fig. 5D), formed when a plasmid containing the

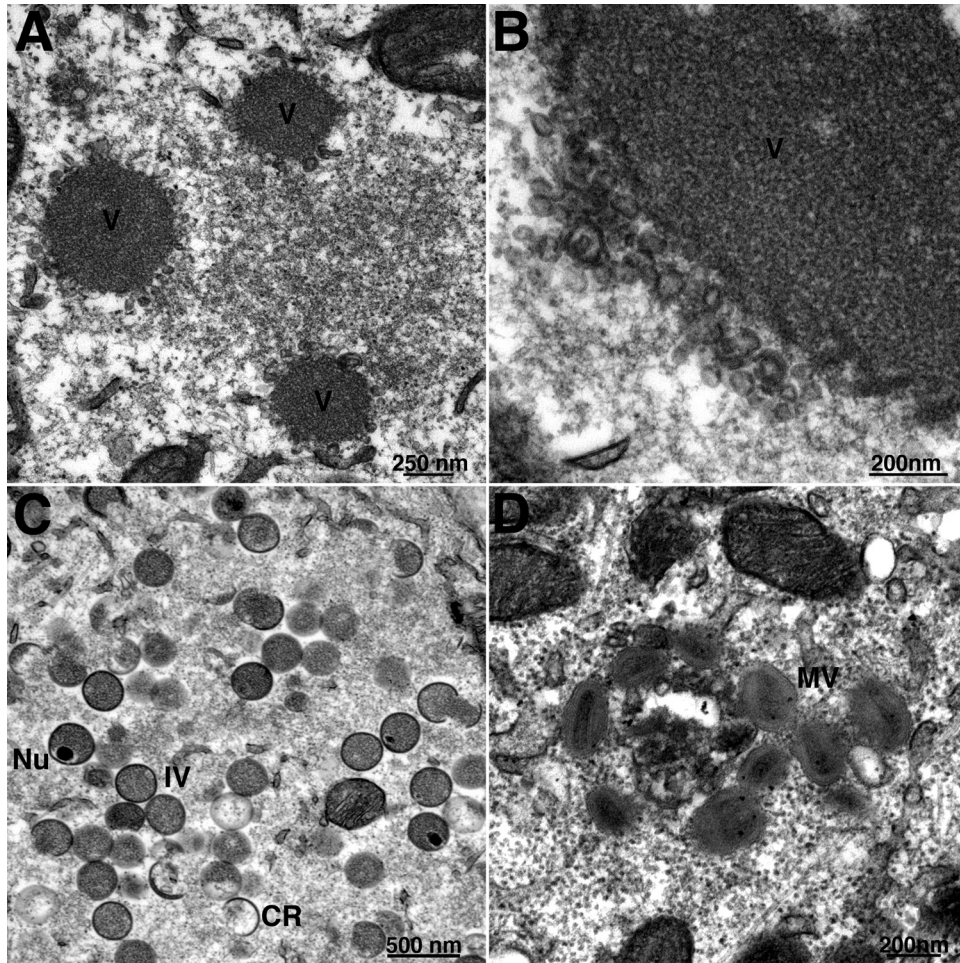


FIG. 5. Complementation of vA17Li morphogenesis by truncated A17 proteins. Transmission electron microscopic images of cells infected with 3 PFU of vA17Li per cell in the absence of IPTG and not transfected (A, B) or transfected with plasmids expressing full-length A17 (C and D), A17Δ160-203 (E), A17Δ1-60 (F), A17Δ1-38 (G, H), or A17Δ1-16 (I, J). CR, crescent; Nu, IV with nucleoid; V, dense viroplasm.

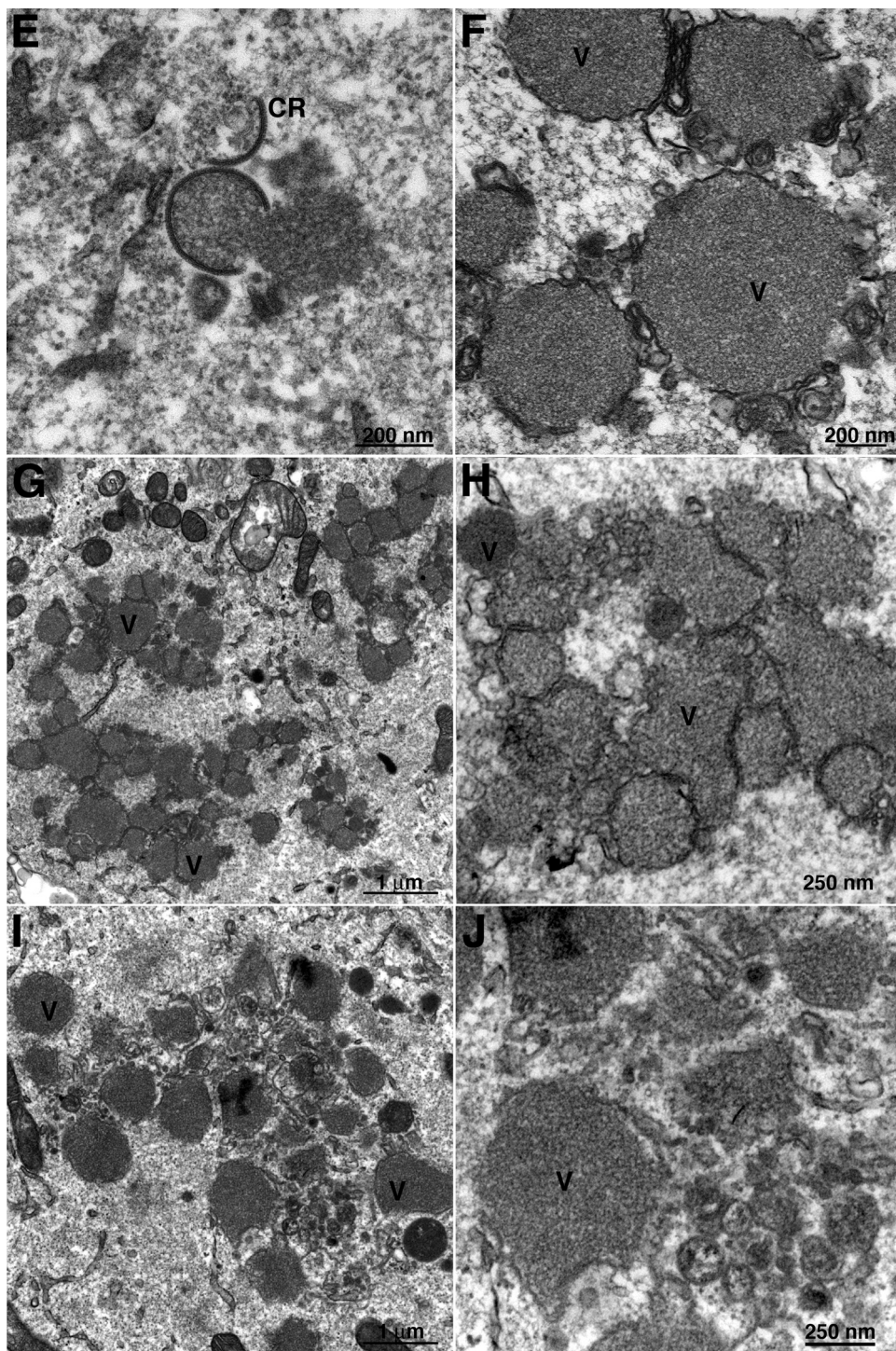


FIG. 5—Continued.

full-length A17 was transfected, consistent with the complementation of infectivity. Plasmid A17Δ160-203 permitted the formation of crescents with the typical outer “spicule layer”; however, these did not progress to completed IVs or MVs (Fig. 5E), indicating that the C terminus was needed for later stages of morphogenesis. No crescents or IVs formed when plasmids expressing any of the N-terminally truncated proteins were

transfected. In each case, there were electron-dense masses surrounded by irregular membranes without the “spicule layer” (Fig. 5F to J), reminiscent of structures seen in rifampin-treated cells and absent from the untransfected cells (Fig. 5A and B). The results for A17Δ1-60 and A17Δ1-38 were consistent with failure of these N-terminal truncated proteins to bind D13. However, a similar phenotype was also found for A17Δ1-

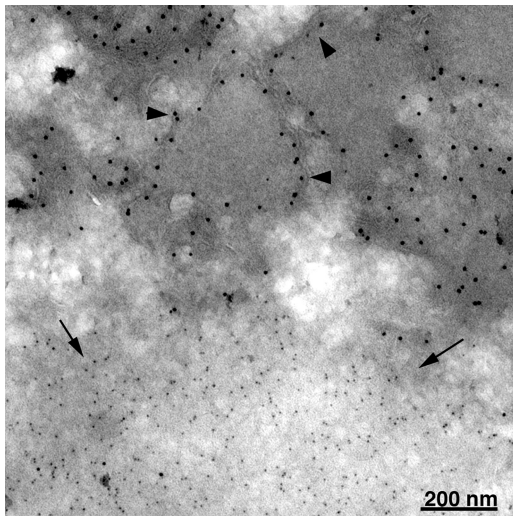


FIG. 6. Localization of N-terminally truncated A17 and D13 by immunoelectron microscopy. BS-C-1 cells were infected with vA17Li in the absence of IPTG and cotransfected with plasmids expressing A17Δ1-60 and D13. After 24 h, the cells were fixed, cryosectioned, and incubated successively with A17C antibody and then protein A conjugated to 10-nm gold particles followed by D13 antibody and then protein A conjugated to 5-nm gold particles. Arrowheads and arrows point to 10- and 5-nm gold particles, respectively.

16, which was shown to be associated with D13 in detergent-treated lysates. Therefore, the extreme N terminus of A17 may play a role in binding to D13 when A17 is embedded in the membrane or these N-terminal amino acids may have an additional role in assembly of the crescents.

Since N-terminally truncated A17 did not induce the formation of crescent and IV structures, we needed to confirm its expression and location relative to D13. Cells were infected with vA17Li without inducer and transfected with plasmids expressing A17Δ1-60 and D13. The cells were fixed, and cryosections were stained with antibody to the C terminus of A17 followed by protein A conjugated to 10-nm gold particles and then with antibody to D13 followed by protein A conjugated to 5-nm gold particles. The N-terminally truncated A17 was associated with irregular membranes surrounding electron-dense substance and distinct from inclusions of D13 (Fig. 6). In contrast, when full-length or C-terminally truncated A17 was expressed, A17 and D13 were both associated with crescent and IV membranes (not shown).

Removal of D13 during morphogenesis requires expression of the I7 protease. In contrast to the results for crescents and IVs, D13 can barely be detected in MVs by immunogold labeling (40). In addition, the lattice structure of the scaffold cannot be visualized in MVs (20). Thus, the scaffold appears to disassemble during morphogenesis. Since our studies indicated that the N-terminal region of A17 is required for the association of the D13 scaffold with viral membranes, we considered that proteolytic processing of A17 might be directly or indirectly involved in its removal. VACV encodes two proteases, I7 and G1. I7 is responsible for the processing of the N and C termini of A17 (2), as well as several core proteins (2, 9). The substrate of G1 is not known, although it may be responsible for self-cleavage (3, 19). Importantly, G1 is not required for

cleavage of A17. Despite their different substrate specificities, the repression of either protease results in the formation of IVs, but further maturation is abnormal and spherical particles with poorly formed cores accumulate. In the present experiments, cells were infected with inducible I7 (2) and G1 (3) viruses in the absence of IPTG. Cryosections of the infected cells were immunogold labeled using rabbit anti-D13 antibody. We found that the IVs were decorated with gold in both cases (Fig. 7A and B). However, D13 staining was detected on the abnormal MVs formed when I7 was repressed (Fig. 7C) but not when G1 was repressed (Fig. 7D). As expected, the D13 staining was absent from MVs in the presence of IPTG (data not shown). Thus, the removal of D13 correlated with I7 protease activity.

Disassembly of the D13 scaffold is prevented by mutation of the N-terminal cleavage site. The results obtained by repression of I7 supported a model that the processing of A17 is involved in the disassembly of the D13 scaffold. However, I7 is responsible for processing at both the N and C termini of A17, as well as for the processing of several core proteins. In order to test the model more specifically, we separately mutated the N- and C-terminal AG/X motifs to AAX, which prevents the cleavage of A17 by I7 protease (2). Plasmids containing unmutated A17 or the AAX mutants regulated by a synthetic early/late VACV promoter were transfected into cells that had been infected with the A17-inducible vA17Li in the absence of IPTG. Some complementation of infectivity occurred with the C-terminal cleavage site mutant A17G185A, but none was detected with the N-terminal mutant A17G16A or with the control GFP plasmid (Fig. 8).

Electron microscopy was carried out to determine the effects of the cleavage site mutations on morphogenesis. Immature and mature viral forms were evident when the unmutated A17 was expressed by transfection of cells infected with vA17Li in the absence of IPTG (Fig. 9A and B). The ratio of IVs to MVs was similar when the cells were transfected with unmutated A17 or A17G185A (Fig. 9E and F). In contrast, cells transfected with the A17G16A mutant contained normal-looking IVs (Fig. 9C) but nearly all the more mature forms appeared abnormal (Fig. 9D).

DISCUSSION

The presence of an external honeycomb lattice, comprised of D13 trimers, provides a structural basis for the uniform curvature of viral crescents and the spherical shape and size of the IVs (28, 41). The questions that we addressed in the present study were how the D13 trimers associate with the nascent viral membrane to form the scaffold and how they are subsequently disassembled to allow further steps in morphogenesis. We took two complementary approaches to answer the first question. One was to engineer a recombinant virus with an epitope tag on D13 and immunoaffinity purify it along with associated proteins from infected cells that were lysed with a detergent to solubilize membranes. This experiment and additional transfection complementation studies provided evidence that A17, an essential transmembrane component of the IV membrane, associated specifically with D13 even in the absence of other viral late proteins and viral membranes. The second approach was immunogold labeling of

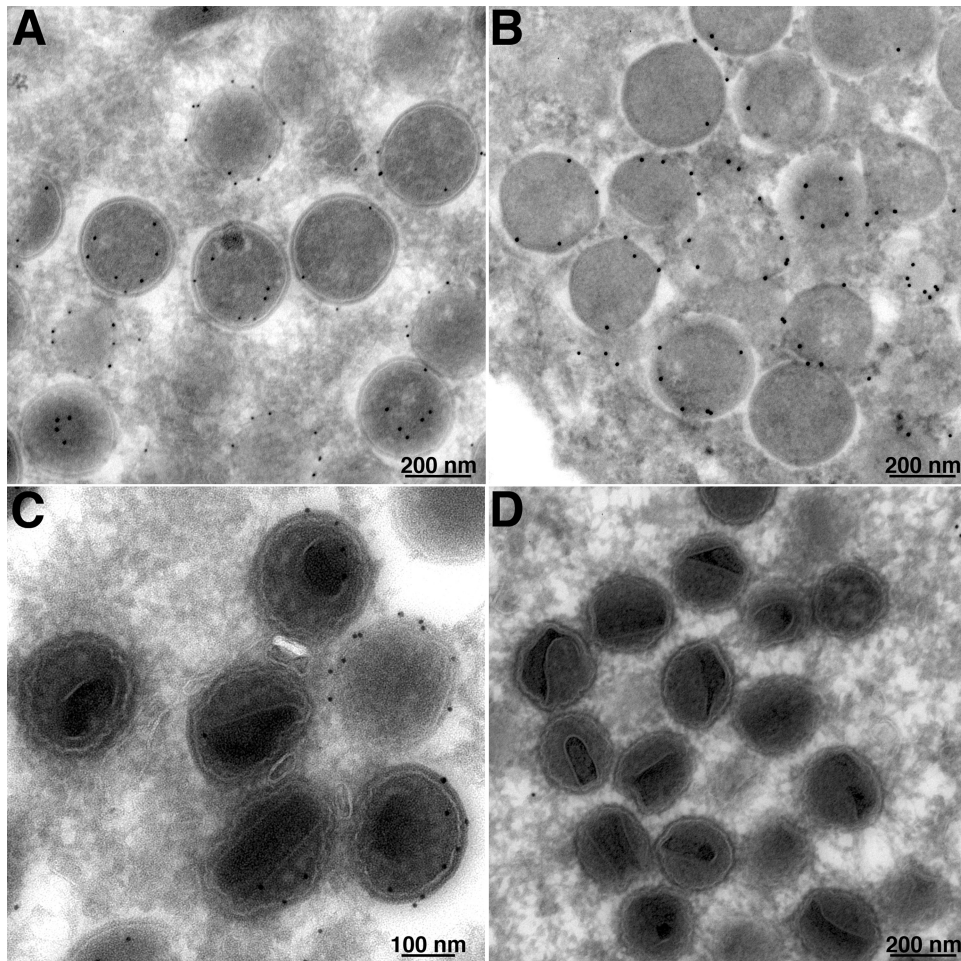


FIG. 7. Immunoelectron microscopy of cells infected with conditionally lethal I7 and G1 mutants. Cells were infected with 3 PFU per cell of vI7Li (A, C) or vG1Li (B, D) in the absence of IPTG. After 24 h, cells were fixed, cryosectioned, and incubated with anti-D13 antibody followed by protein A conjugated to colloidal gold. Images of fields containing IVs (A, B) and more mature forms (C, D) are shown.

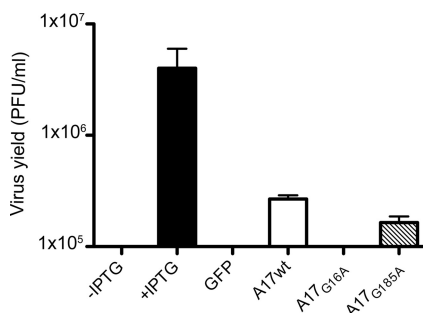


FIG. 8. Complementation of vA17Li infectivity by A17 cleavage site mutants. Cells were infected with 5 PFU of vA17Li in the presence of IPTG (+IPTG) or absence of IPTG (all other lanes) and either not transfected (first lane) or transfected with a plasmid expressing GFP, full-length (wild type) A17 (A17wt), or mutated A17 in which glycine 16 or 185 was replaced by alanine regulated by a synthetic early/late promoter. The cells were harvested after 24 h, and virus titers were determined by plaque assay in the presence of 100 μ M IPTG. Error bars show standard deviations.

thawed cryosections of infected cells to localize D13 and other viral proteins by transmission electron microscopy. D13 and A17 were closely associated in vesicular structures when viral membrane formation was impaired by repressing synthesis of the A14 protein. In contrast, when synthesis of A17 was repressed, D13 was present in separate depots rather than the tubulovesicular structures containing A14. Normally, D13 must associate very quickly with A17 and the nascent viral membrane, since even small crescents seem to be mostly coated, although uncoated ends are sometimes visible. Nevertheless, “naked” viral membranes can form without the interaction of D13, as occurs in the presence of rifampin or with a D13 conditionally lethal mutant. Rifampin removal experiments demonstrate that the irregular membranes are coated with D13 within minutes (29).

The A17 protein of the WR strain of VACV is encoded by ORF 137, which predicts a 203-amino-acid polypeptide with a largely hydrophobic central region. In vitro studies with microsome-supplemented reticulocyte extracts indicated that A17 is cotranslationally inserted into membranes with the N- and C-terminal segments exposed to the cytoplasm (25) and two membrane-spanning domains (5, 6). Although A17 and D13

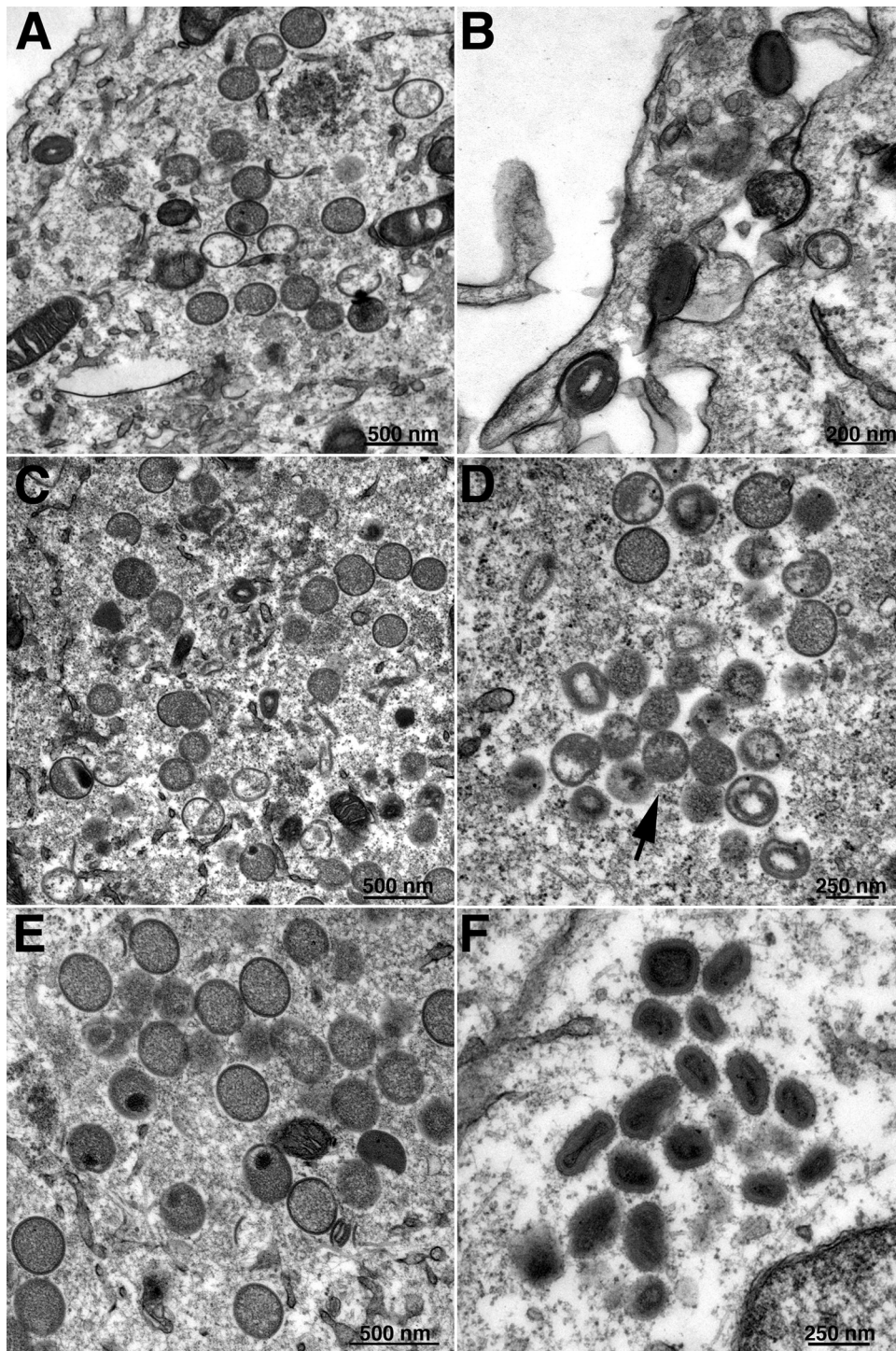


FIG. 9. Complementation of vA17Li morphogenesis by A17 cleavage site mutants. Cells were infected with vA17Li in the absence of IPTG and transfected with plasmids expressing full-length A17 (A, B), A17G16A (C, D), or A17G185A (E, F) as described in the legend of Fig. 8. After 22 h, the cells were prepared for transmission electron microscopy. Images of fields containing IVs (A, C, E) and more mature forms (B, D, F) are shown. The arrow in panel D points to a cluster of abnormal virions.

were both reported to line the concave side of crescent and IV membranes (25, 40), other studies indicated that this interpretation resulted from image superimposition and that both D13 and A17 are on the outer surface (28, 41). Thus, A17 is posi-

tioned to associate with the outer scaffold. Antibodies to both ends of unprocessed A17 were shown to decorate IVs (25), and in view of the topology of A17, it seemed likely that the N- or C-terminal segment would interact with D13. Immunoaffinity

purification studies demonstrated that the entire C-terminal segment of A17 could be removed without preventing association with D13, whereas removal of the entire N-terminal segment abrogated the interaction. These data correlated with the effect of truncation mutations on the formation of crescents and IVs, which occurred with the C-terminal truncation but not with the N-terminal truncation. With the latter mutant, irregular membranes formed at the periphery of inclusions containing electron-dense granular material called viroplasm. These structures closely resemble the irregular membranes formed in the presence of rifampin (18, 29, 30) or when the expression of D13 is repressed (50). Presumably the central region of A17, which is largely comprised of membrane-spanning domains, participates in the formation of the viral membrane. Binding to D13 still occurred when amino acids 1 to 16 of A17 were deleted, but not when amino acids 1 to 38 were removed, suggesting that at least part of the D13 binding region of A17 lies between amino acids 16 and 38. Nevertheless, truncation of amino acids 1 to 16 or 1 to 38 of A17 each resulted in the formation of irregular membranes instead of crescents and IVs. It is possible that when A17 is embedded in the viral membrane, the N-terminal 16 amino acids of A17 are also required for binding to D13. Alternatively, the N terminus of A17 may have an additional role in assembly.

We have not yet carried out mutagenesis studies of D13 to determine which part(s) interacts with A17. However, a single substitution of glycine for aspartic acid 513 near the C terminus of D13 results in the spontaneous formation of flat lattice structures that fail to associate with viral membranes (41). In addition, D13 fails to interact with viral crescents in the presence of rifampin and the majority of mutations that confer rifampin resistance occur near the N and C termini (4, 11, 42). The proximity of the N and C termini of the ORF virus homolog of D13 with the viral membrane is consistent with the structure obtained by electron microscopy of two-dimensional crystals (22) when fitted with the higher-resolution structure of VP54, the major capsid protein of *Paramecium bursaria Chlorella* virus type 1 (31). In addition, the N-terminal region of the capsid protein of phage PRD-1 interacts with the underlying membrane (1).

The second question posed in this study is how the scaffold is disassembled to allow IVs to morph into MVs. In contrast to IVs, MVs cannot be immunogold labeled to a significant degree with antibody to D13, suggesting that most of the D13 is removed, although some can still be detected in purified MVs by biochemical methods (33, 40). Our results suggest that the disassembly of the D13 scaffold is related to the processing of A17. A17 is processed by proteolytic cleavage and phosphorylation (15, 35). The protease encoded by the VACV I7L gene can cleave A17 at amino acids 16 or 18 near the N terminus and at amino acid 185 near the C terminus (2). When the expression of the I7 protease is repressed, cleavage of A17, as well as certain core proteins, is inhibited and the maturation of IVs is perturbed (2, 10). Under the latter conditions, large numbers of dense particles that are more spherical than MVs accumulate. Here we showed by immunoelectron microscopy that these particles, unlike MVs, retained D13. Although virus particles that formed when the G1 protease was repressed did not attain the oval shape or characteristic core structure of MVs, A17 was cleaved (3) and we detected very little D13. To

further correlate A17 cleavage and removal of the scaffold, transfection/complementation studies were carried out using A17 with mutations of the AG/X sites near the N and C termini of A17. A17 with the C-terminal AG/X mutated still complemented the infectivity of the inducible A17 virus, although to a lesser extent than the unmutated form. In addition, both IVs and MVs were seen by transmission electron microscopy. In contrast, mutation of the N-terminal AG/X site completely prevented complementation of infectivity; normal IVs but only abnormal-looking more-mature forms were seen. Thus, disassembly of the IV scaffold was correlated with cleavage of the N terminus of A17 by the I7 protease. Precisely how the scaffold is removed and whether D13 is degraded or recycled remains to be determined.

ACKNOWLEDGMENTS

We thank Paula Traktman for providing the A14-inducible VACV and Catherine Cotter for tissue culture cells.

The research was supported by the Division of Intramural Research, National Institute of Allergy and Infectious Diseases, National Institutes of Health.

REFERENCES

- Abrescia, N. G., J. J. Cockburn, J. M. Grimes, G. C. Sutton, J. M. Diprose, S. J. Butcher, S. D. Fuller, C. San Martin, R. M. Burnett, D. I. Stuart, D. H. Bamford, and J. K. Bamford. 2004. Insights into assembly from structural analysis of bacteriophage PRD1. *Nature* **432**:68–74.
- Ansarah-Sobrinho, C., and B. Moss. 2004. Role of the I7 protein in proteolytic processing of vaccinia virus membrane and core components. *J. Virol.* **78**:6335–6343.
- Ansarah-Sobrinho, C., and B. Moss. 2004. Vaccinia virus G1 protein, a predicted metalloprotease, is essential for morphogenesis of infectious virions but not for cleavage of major core proteins. *J. Virol.* **78**:6855–6863.
- Baldick, C. J., and B. Moss. 1987. Resistance of vaccinia virus to rifampicin conferred by a single nucleotide substitution near the predicted NH₂ terminus of a gene encoding an M_r 62,000 polypeptide. *Virology* **156**:138–145.
- Betakova, T., and B. Moss. 2000. Disulfide bonds and membrane topology of the vaccinia virus A17L envelope protein. *J. Virol.* **74**:2438–2442.
- Betakova, T., E. J. Wolfe, and B. Moss. 1999. Membrane topology of the vaccinia virus A17L envelope protein. *Virology* **261**:347–356.
- Betakova, T., E. J. Wolfe, and B. Moss. 1999. Regulation of vaccinia virus morphogenesis: phosphorylation of the A14L and A17L membrane proteins and C-terminal truncation of the A17L protein are dependent on the F10L protein kinase. *J. Virol.* **73**:3534–3543.
- Bisht, H., A. S. Weisberg, and B. Moss. 2008. Vaccinia virus L1 protein is required for cell entry and membrane fusion. *J. Virol.* **82**:8687–8694.
- Byrd, C. M., T. C. Bolken, and D. E. Hruby. 2002. The vaccinia virus I7L gene product is the core protein proteinase. *J. Virol.* **76**:8973–8976.
- Byrd, C. M., and D. E. Hruby. 2005. A conditional-lethal vaccinia virus mutant demonstrates that the I7L gene product is required for virion morphogenesis. *Virol. J.* **2**:4.
- Charity, J. C., E. Katz, and B. Moss. 2007. Amino acid substitutions at multiple sites within the vaccinia virus D13 scaffold protein confer resistance to rifampicin. *Virology* **359**:227–232.
- da Fonseca, F. G., E. J. Wolfe, A. Weisberg, and B. Moss. 2000. Characterization of the vaccinia virus H3L envelope protein: topology and posttranslational membrane insertion via the C-terminal hydrophobic tail. *J. Virol.* **74**:7508–7517.
- da Fonseca, F. G., E. J. Wolfe, A. Weisberg, and B. Moss. 2000. Effects of deletion or stringent repression of the H3L envelope gene on vaccinia virus replication. *J. Virol.* **74**:7518–7528.
- Dales, S., and E. H. Mosbach. 1968. Vaccinia as a model for membrane biogenesis. *Virology* **35**:564–583.
- Derrien, M., A. Punjabi, R. Khanna, O. Grubisha, and P. Traktman. 1999. Tyrosine phosphorylation of A17 during vaccinia virus infection: involvement of the H1 phosphatase and the F10 kinase. *J. Virol.* **73**:7287–7296.
- De Silva, F. S., W. Lewis, P. Berglund, E. V. Koonin, and B. Moss. 2007. Poxvirus DNA primase. *Proc. Natl. Acad. Sci. USA* **104**:18724–18729.
- Earl, P. L., B. Moss, L. S. Wyatt, and M. W. Carroll. 1998. Generation of recombinant vaccinia viruses, p. 16.17.1–16.17.19. In F. M. Ausubel, R. Brent, R. E. Kingston, D. D. Moore, J. G. Seidman, J. A. Smith, and K. Struhl (ed.), *Current protocols in molecular biology*, vol. 2. Greene Publishing Associates & Wiley Interscience, New York, NY.
- Grimley, P. M., E. N. Rosenblum, S. J. Mims, and B. Moss. 1970. Inter-

- ruption by rifampin of an early stage in vaccinia virus morphogenesis: accumulation of membranes which are precursors of virus envelopes. *J. Virol.* **6**:519–533.
19. Hedengren-Olcott, M., C. M. Byrd, J. Watson, and D. E. Hruby. 2004. The vaccinia virus G1L putative metalloproteinase is essential for viral replication in vivo. *J. Virol.* **78**:9947–9953.
 20. Heuser, J. 2005. Deep-etch EM reveals that the early poxvirus envelope is a single membrane bilayer stabilized by a geodetic “honeycomb” surface coat. *J. Cell Biol.* **169**:269–283.
 21. Husain, M., A. S. Weisberg, and B. Moss. 2006. Existence of an operative pathway from the endoplasmic reticulum to the immature poxvirus membrane. *Proc. Natl. Acad. Sci. USA* **103**:19506–19511.
 22. Hyun, J. K., F. Coulibaly, A. P. Turner, E. N. Baker, A. A. Mercer, and A. K. Mitra. 2007. The structure of a putative scaffolding protein of immature poxvirus particles as determined by electron microscopy suggests similarity with capsid proteins of large icosahedral DNA viruses. *J. Virol.* **81**:11075–11083.
 23. Iyer, L. A., S. Balaji, E. V. Koonin, and L. Aravind. 2006. Evolutionary genomics of nucleo-cytoplasmic large DNA viruses. *Virus Res.* **117**:156–184.
 24. Iyer, L. M., L. Aravind, and E. V. Koonin. 2001. Common origin of four diverse families of large eukaryotic DNA viruses. *J. Virol.* **75**:11720–11734.
 25. Krijnse-Locker, J., S. Schleich, D. Rodriguez, B. Goud, E. J. Snijder, and G. Griffiths. 1996. The role of a 21-kDa viral membrane protein in the assembly of vaccinia virus from the intermediate compartment. *J. Biol. Chem.* **271**:14950–14958.
 26. Lin, C. L., C. S. Chung, H. G. Heine, and W. Chang. 2000. Vaccinia virus envelope H3L protein binds to cell surface heparan sulfate and is important for intracellular mature virion morphogenesis and virus infection in vitro and in vivo. *J. Virol.* **74**:3353–3365.
 27. Lustig, S., C. Fogg, J. C. Whitbeck, R. J. Eisenberg, G. H. Cohen, and B. Moss. 2005. Combinations of polyclonal or monoclonal antibodies to proteins of the outer membranes of the two infectious forms of vaccinia virus protect mice against a lethal respiratory challenge. *J. Virol.* **79**:13454–13462.
 28. Mohandas, A. R., and S. Dales. 1995. Involvement of spicules in the formation of vaccinia virus envelopes elucidated by a conditional lethal mutant. *Virology* **214**:494–502.
 29. Moss, B., E. N. Rosenblum, E. Katz, and P. M. Grimley. 1969. Rifampicin: a specific inhibitor of vaccinia virus assembly. *Nature* **224**:1280–1284.
 30. Nagayama, A., B. G. T. Pogo, and S. Dales. 1970. Biogenesis of vaccinia: separation of early stages from maturation by means of rifampicin. *Virology* **40**:1039–1051.
 31. Nandhagopal, N., A. A. Simpson, J. R. Gurnon, X. Yan, T. S. Baker, M. V. Graves, J. L. Van Etten, and M. G. Rossmann. 2002. The structure and evolution of the major capsid protein of a large, lipid-containing DNA virus. *Proc. Natl. Acad. Sci. USA* **99**:14758–14763.
 32. Nelson, G. E., J. R. Sisler, D. Chandran, and B. Moss. 2008. Vaccinia virus entry/fusion complex subunit A28 is a target of neutralizing and protective antibodies. *Virology* **380**:394–401.
 33. Resch, W., K. K. Hixson, R. J. Moore, M. S. Lipton, and B. Moss. 2007. Protein composition of the vaccinia virus mature virion. *Virology* **358**:233–247.
 34. Rodríguez, D., M. Esteban, and J. R. Rodríguez. 1995. Vaccinia virus A17L gene product is essential for an early step in virion morphogenesis. *J. Virol.* **69**:4640–4648.
 35. Rodriguez, D., J. R. Rodriguez, and M. Esteban. 1993. The vaccinia virus 14-kilodalton fusion protein forms a stable complex with the processed protein encoded by the vaccinia virus A17L gene. *J. Virol.* **67**:3435–3440.
 36. Rodriguez, J. R., C. Risco, J. L. Carrascosa, M. Esteban, and D. Rodriguez. 1997. Characterization of early stages in vaccinia virus membrane biogenesis: implications of the 21-kilodalton protein and a newly identified 15-kilodalton envelope protein. *J. Virol.* **71**:1821–1833.
 37. Rodriguez, J. R., C. Risco, J. L. Carrascosa, M. Esteban, and D. Rodriguez. 1998. Vaccinia virus 15-kilodalton (A14L) protein is essential for assembly and attachment of viral crescents to virosomes. *J. Virol.* **72**:1287–1296.
 38. Senkevich, T. G., B. M. Ward, and B. Moss. 2004. Vaccinia virus entry into cells is dependent on a virion surface protein encoded by the A28L gene. *J. Virol.* **78**:2357–2366.
 39. Senkevich, T. G., L. S. Wyatt, A. S. Weisberg, E. V. Koonin, and B. Moss. 2008. A conserved poxvirus NlpC/P60 superfamily protein contributes to vaccinia virus virulence in mice but not to replication in cell culture. *Virology* **374**:506–514.
 40. Sodeik, B., G. Griffiths, M. Ericsson, B. Moss, and R. W. Doms. 1994. Assembly of vaccinia virus: effects of rifampicin on the intracellular distribution of viral protein p65. *J. Virol.* **68**:1103–1114.
 41. Szajner, P., A. S. Weisberg, J. Lebowitz, J. Heuser, and B. Moss. 2005. External scaffold of spherical immature poxvirus particles is made of protein trimers, forming a honeycomb lattice. *J. Cell Biol.* **170**:971–981.
 42. Tartaglia, J., A. Piccini, and E. Paoletti. 1986. Vaccinia virus rifampicin-resistance locus specifies a late 63,000 Da gene product. *Virology* **150**:45–54.
 43. Traktman, P., K. Liu, J. DeMasi, R. Rollins, S. Jesty, and B. Unger. 2000. Elucidating the essential role of the A14 phosphoprotein in vaccinia virus morphogenesis: construction and characterization of a tetracycline-inducible recombinant. *J. Virol.* **74**:3682–3695.
 44. Ward, G. A., C. K. Stover, B. Moss, and T. R. Fuerst. 1995. Stringent chemical and thermal regulation of recombinant gene expression by vaccinia virus vectors in mammalian cells. *Proc. Natl. Acad. Sci. USA* **92**:6773–6777.
 45. Wolfe, E. J., D. M. Moore, P. J. Peters, and B. Moss. 1996. Vaccinia virus A17L open reading frame encodes an essential component of nascent viral membranes that is required to initiate morphogenesis. *J. Virol.* **70**:2797–2808.
 46. Wolfe, E. J., S. Vijaya, and B. Moss. 1995. A myristylated membrane protein encoded by the vaccinia virus L1R open reading frame is the target of potent neutralizing monoclonal antibodies. *Virology* **211**:53–63.
 47. Xiao, C., P. R. Chipman, A. J. Battisti, V. D. Bowman, P. Renesto, D. Raoult, and M. G. Rossmann. 2005. Cryo-electron microscopy of the giant mimivirus. *J. Mol. Biol.* **353**:493–496.
 48. Yan, X., N. H. Olson, J. L. Van Etten, M. Bergoin, M. G. Rossmann, and T. S. Baker. 2000. Structure and assembly of large lipid-containing dsDNA viruses. *Nat. Struct. Biol.* **7**:101–103.
 49. Yan, X., Z. Yu, P. Zhang, A. J. Battisti, H. A. Holdaway, P. R. Chipman, C. Bajaj, M. Bergoin, M. G. Rossmann, and T. S. Baker. 2009. The capsid proteins of a large, icosahedral dsDNA virus. *J. Mol. Biol.* **385**:1287–1299.
 50. Zhang, Y., and B. Moss. 1992. Immature viral envelope formation is interrupted at the same stage by lac operator-mediated repression of the vaccinia virus D13L gene and by the drug rifampicin. *Virology* **187**:643–653.